Organic LETTERS

Letter

pubs.acs.org/OrgLett

Porphyrin–Polyyne [3]- and [5]Rotaxanes

Daniel R. Kohn, Levon D. Movsisyan, Amber L. Thompson, and Harry L. Anderson*

University of Oxford, Department of Chemistry, Chemistry Research Laboratory, Oxford OX1 3TA, United Kingdom

Supporting Information

ABSTRACT: Porphyrin–polyyne [3]- and [5]rotaxanes have been synthesized by condensing aldehyde–rotaxanes with pyrrole or dipyrromethane. The crystal structure of a [3]rotaxane shows that the macrocycles adopt compact conformations, holding the hexaynes near the porphyrin core, and that the phenanthroline units form intermolecular π-stacked dimers in the solid. Fluorescence spectra reveal singlet excited-state energy transfer from the threaded hexayne to the porphyrin, from the phenanthroline to the porphyrin, and from the phenanthroline to the hexayne.

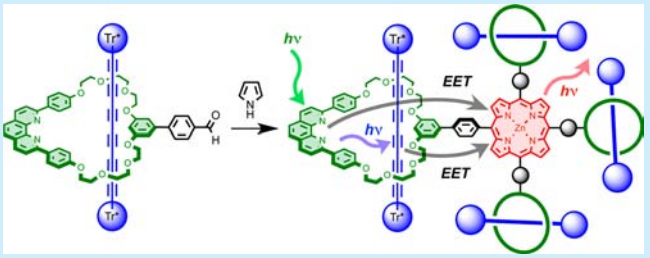

Macrocycles consisting entirely of sp-hydridized carbon are intriguing synthetic targets.[1−3] Cyclocarbons have been studied in the gas phase,[1,2,4] but they have not yet been isolated or characterized in solution, despite attempts by Diederich, Tobe, Rees, and co-workers.[1−3] Advances in active metal template synthesis[5] provide access to an expanding diversity of interlocked molecules, including threaded polyynes,[6−11] and it has been found that linear chains of sp-hybridized carbon atoms (both polyynes and cumulenes) can be stabilized by threading them through macrocycles to form rotaxanes.[11−13] As part of a project directed toward the synthesis of cyclocarbon catenanes, we are exploring strategies for positioning several polyyne rotaxane units around a central molecular hub, so that the polyynes can then be linked together to form a threaded cyclocarbon. Here, we present the first step in this endeavor: the synthesis of a [5]rotaxane in which four hexaynes are positioned around a porphyrin core. While the primary motivation for this work was to explore approaches to cyclocarbon catenanes, this study also provides insights into the interactions between the singlet excited states of polyyne and porphyrin chromophores.

The initial target of this work was the porphyrin [5]rotaxane **P5Ra** shown in Figure 1. All attempts at the synthesis of this [5]rotaxane failed, presumably as a consequence of the steric bulk of the four [2]rotaxane substituents. However, we successfully synthesized the analogous porphyrin [5]rotaxane **P5Rb** with *p*-phenylene spacers at the *meso*-positions and the corresponding porphyrin [3]rotaxanes **P3Ra** and **P3Rb** (Scheme 1). Here, we present the synthesis of these rotaxanes and an analysis of their fluorescence behavior, together with the crystal structure of a porphyrin [3]rotaxane **P3Ra**. This structure shows that the macrocycles adopt compact conformations due to the predominantly gauche geometries of the O–CH_2CH_2–O links, which increases the effective steric bulk of the rotaxane substituents and explains why the [5]rotaxane **P5Ra** could not be synthesized.

Our synthetic approach starts with the macrocyclic aldehyde **Ma** (Scheme 1).[14,15] Active metal template Cadiot–Chodkiewicz coupling[7,11] of supertrityl triyne Tr*C_6H and bromotriyne Tr*C_6Br [where Tr* is tris(3,5-di-*tert*-butylphenyl)methyl[16]] in the presence of the copper(I) complex of **Ma** gave the [2]rotaxane aldehyde **2Ra** in 58% yield. A wide variety of conditions were tested for the reaction of **2Ra** with pyrrole in attempts to prepare **P5Ra**, but they all failed to give even a trace of this target [5]rotaxane, whereas control reactions of aldehyde **Ma** produced porphyrin **PM4a** in good yield. In contrast, reaction of the rotaxane aldehyde **2Ra** with dipyrromethane gave the porphyrin [3]rotaxane **P3Ra** in 62% yield. These results

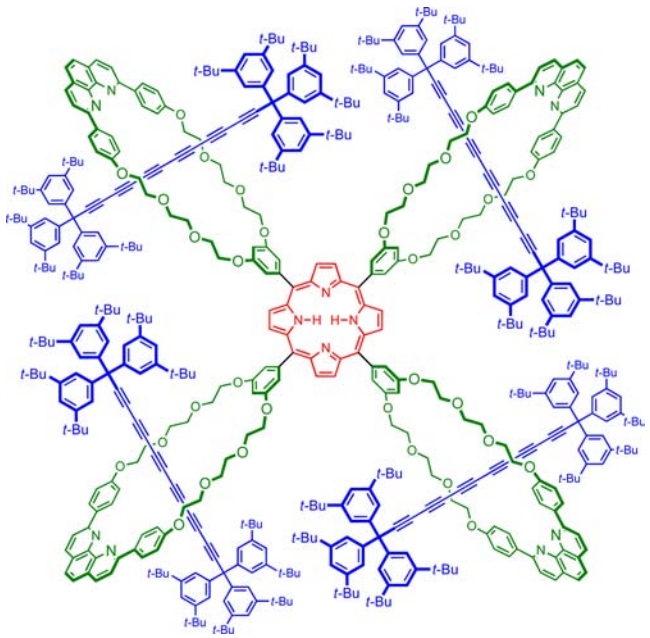

Figure 1. Structure of target [5]rotaxane **P5Ra**.

Received: November 26, 2016
Published: January 5, 2017

DOI: 10.1021/acs.orglett.6b03528
Org. Lett. 2017, 19, 348–351

Scheme 1. Polyrotaxane and Porphyrin Synthesis[a]

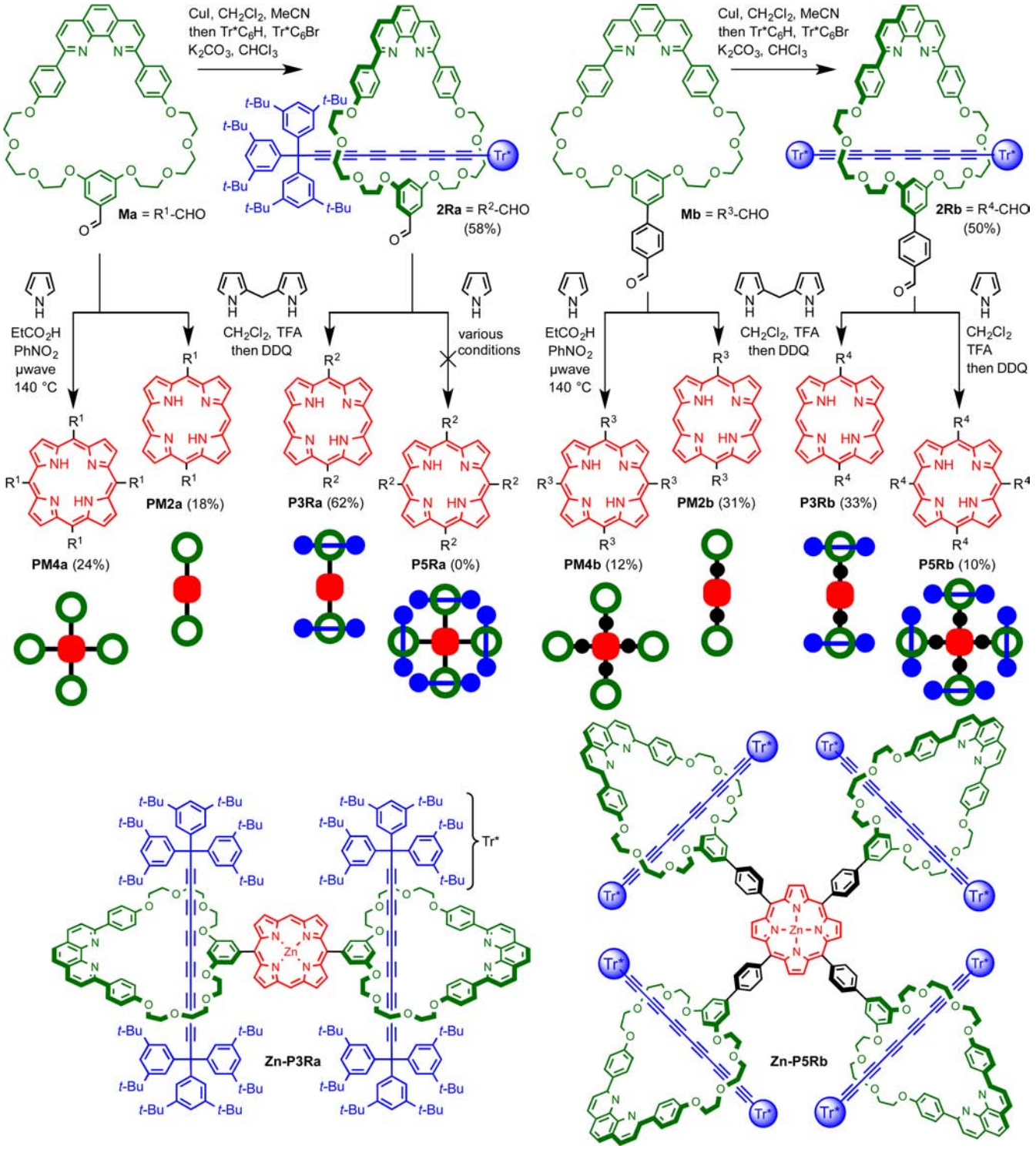

[a]Porphyrins **PM4a**, **PM2a**, **P3Ra**, **P5Ra**, **PM4b**, **PM2b**, **P3Rb**, and **P5Rb** were isolated as zinc complexes after treatment with $Zn(OAc)_2 \cdot 2H_2O$ in methanol/chloroform.

imply that formation of **P5Ra** is blocked by the steric bulk of the rotaxane units, so we investigated the analogous compounds derived from macrocycle **Mb**, which has a *p*-phenylene spacer between the aldehyde functionality and the macrocycle. Increasing the distance between the bulky rotaxane unit and the porphyrin hub made it possible to synthesize [5]rotaxane **P5Rb** (10% yield isolated).

The porphyrin [3]- and [5]rotaxanes, and reference porphyrins, were fully characterized as their zinc complexes **Zn−P3Ra**, **Zn−P3Rb**, **Zn−P5Rb**, **Zn−PM2a**, **Zn−PM4a**, **Zn−PM2b**, and **Zn−PM4b** (see the Supporting Information). Crystals of **Zn−P3Ra** were grown by diffusion of methanol vapor into a solution in chloroform and analyzed by single-crystal X-ray diffraction.[17] The crystal structure has two molecules of

DOI: 10.1021/acs.orglett.6b03528
Org. Lett. 2017, 19, 348−351

Zn−P3Ra in the asymmetric unit; both rotaxane molecules have similar conformations with methanol coordinated to the zinc centers. The phenanthroline units of each rotaxane form intermolecular π-stacked dimers with crystallographically equivalent rotaxanes, forming infinite strands of interactions, as illustrated in Figure 2. The oligoethylene glycol chains of the

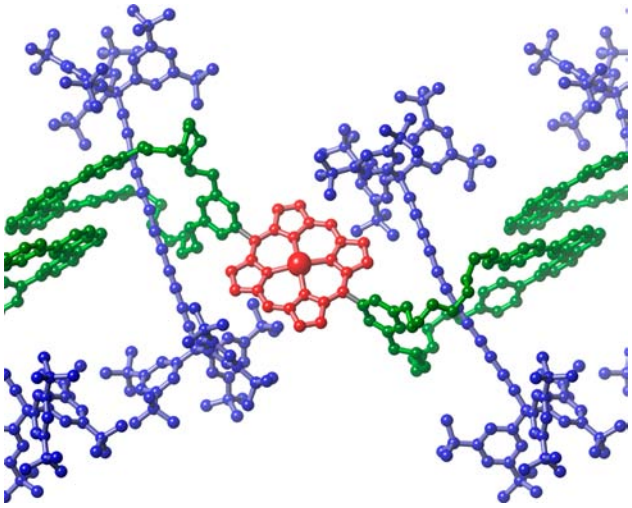

Figure 2. Projection of the structure of the [3]rotaxane **Zn−P3Ra** from X-ray crystallography. This figure only shows one of the two molecules in the asymmetric unit.

macrocycles adopt compact conformations and are mostly gauche (O−CH_2CH_2−O torsional angle 40−80°) with the polyyne chains held close to the porphyrin units. Thus, all four polyyne chains in the asymmetric unit make van der Waals contacts with the β-pyrrole protons of the porphyrins (sp-C···H distance: 2.9−3.1 Å). The hexayne chains have slightly curved geometries, similar to those reported in crystal structures of other polyynes.[9,11,16,18−20]

The family of rotaxanes synthesized during this study provides a unique opportunity to investigate photophysical interactions between the excited states of polyyne and porphyrin chromophores. The photophysical behavior of polyynes is particularly interesting because their absorption spectra are dominated by strong transitions to higher excited states at 280−320 nm (S_0−S_n, $\varepsilon \approx 3 \times 10^5$ M^{-1} cm^{-1}); absorption into the first excited state is dipole-forbidden and can occasionally be observed as a very weak band at 350−450 nm (S_0−S_1, $\varepsilon \approx 500$ M^{-1} cm^{-1}).[16,18] Polyynes also exhibit remarkably fast intersystem crossing (S_1−T_1), which usually prevents observation of fluorescence.

The absorption spectra of rotaxanes **Zn−P3Ra**, **Zn−P3Rb**, and **Zn−P5Rb** demonstrate that threading causes very little perturbation to the electronic structure of the component chromophores. Thus, the absorption bands of the polyyne (280−320 nm), the phenanthroline macrocycle (250−380 nm), and porphyrin (400−450 nm Soret band and 530−560 nm Q-band) are readily identified in the rotaxanes. Comparison with simple reference porphyrin derivatives (*meso*-tetraphenyl porphyrin for **Zn−P5Rb** and **Zn−PM4a**; 5,15-diaryl porphyrin for **Zn−P3Ra**, **Zn−P3Rb**, **Zn−PM2a**, and **Zn−PM2b**) shows that the polyyne and phenanthroline macrocycle units have no effect on the fluorescence quantum yield, measured on excitation of the porphyrin Soret band at around 415 nm. This demonstrates that there is no significant energy migration from the porphyrin to the polyyne or to the macrocycle.

Fluorescence excitation spectra of the rotaxanes, measured by recording emission from the porphyrin Q-band at around 640 nm, show clear features from excitation into the polyyne and phenanthroline macrocycle components, as illustrated for **Zn−P3Ra** and **Zn−PM2a** in Figure 3, indicating that both of these

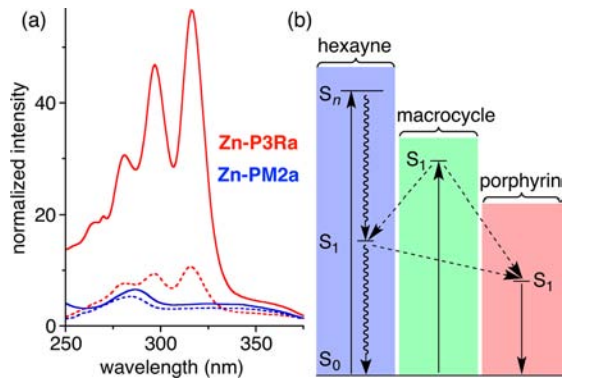

Figure 3. (a) Absorption spectra (continuous line) and excitation spectra (dashed line) of **Zn−P3Ra** (red) and **Zn-PM2a** (blue); the spectral intensities are normalized to 1.0 at the Q-band, and the excitation spectra are recorded for emission at 639 nm (porphyrin Q-band). Solvent: CH_2Cl_2. (b) Jablonski diagram showing the energy-transfer processes.

chromophores transfer energy to the porphyrin. A detailed examination of the absorption spectra, fluorescence spectra, and excitation spectra of the whole family of compounds allowed us to determine the quantum yields of excited-state energy transfer (EET) from the polyyne to the porphyrin and from the phenanthroline macrocycle to the porphyrin as summarized in Table 1 (see the SI for full details).

Table 1. Energy-Transfer Efficiencies ϕ_{EET}

compd	ϕ_{EET}(macrocycle → porphyrin)	ϕ_{EET}(polyyne → porphyrin)
Zn−PM2a	0.67 ± 0.08	
Zn−P3Ra	0.32 ± 0.03	0.16 ± 0.02
Zn−PM2b	0.88 ± 0.11	
Zn−P3Rb	0.22 ± 0.03	0.10 ± 0.03
Zn−PM4b	0.68 ± 0.06	
Zn−P5Rb	0.25 ± 0.02	0.09 ± 0.02

The comparison of macrocycle → porphyrin EET efficiencies in the presence and absence of polyyne show that the polyyne acts as a sink for singlet excited state energy from the phenanthroline macrocycle, even though it does not quench the porphyrin.[18] The excited-state energy of the macrocycle is split between the porphyrin and the polyyne. The higher efficiency of polyyne → porphyrin EET in [3]rotaxane **Zn−P3Ra**, compared with **Zn−P3Rb** and **Zn−P5Rb**, reflects the shorter polyyne−porphyrin distance. The polyyne → porphyrin EET must be very rapid to compete with intersystem crossing ($\tau \approx 0.5$ ns).[18] Furthermore, the S_1 of the polyyne is a dark state with negligible oscillator strength; therefore, Förster-type energy transfer is expected to be very inefficient, implying that the observed EET occurs via a Dexter mechanism.

In conclusion, we have prepared a series of porphyrin−polyyne [3]- and [5]rotaxanes that comprise multiple chromophores in a unique interlocked architecture. An analysis

DOI: 10.1021/acs.orglett.6b03528
Org. Lett. 2017, 19, 348−351

of the absorption, fluorescence, and excitation spectra of the rotaxanes reveals three types of energy-transfer processes (a) from the phenanthroline macrocycle to the porphyrin, (b) from the phenanthroline macrocycle to the polyyne, and (c) from the polyyne to the porphyrin. This work paves the way for a template-directed synthesis of polycatenane cyclo[*n*]carbons.

■ ASSOCIATED CONTENT

Supporting Information

The Supporting Information is available free of charge on the ACS Publications website at DOI: 10.1021/acs.orglett.6b03528.

Details of synthetic procedures and characterization data, analysis of absorption, fluorescence and excitation spectra, and crystallographic analysis (PDF)
Crystallographic data for **P3Ra** (CIF)

■ AUTHOR INFORMATION

Corresponding Author

*E-mail: harry.anderson@chem.ox.ac.uk.

ORCID

Harry L. Anderson: 0000-0002-1801-8132

Notes

The authors declare no competing financial interest.

■ ACKNOWLEDGMENTS

We thank the EPSRC and the European Research Council (Grant No. 320969) for support, the EPSRC UK Mass Spectrometry Facility at Swansea University for mass spectra, and Diamond Light Source for an award of beamtime.

■ REFERENCES

(1) (a) Diederich, F.; Rubin, Y.; Knobler, C. B.; Whetten, R. L.; Schriver, K. E.; Houk, K. N.; Li, Y. *Science* **1989**, *245*, 1088. (b) Rubin, Y.; Diederich, F. *J. Am. Chem. Soc.* **1989**, *111*, 6870. (c) Rubin, Y.; Knobler, C. B.; Diederich, F. *J. Am. Chem. Soc.* **1990**, *112*, 1607. (d) Rubin, Y.; Kahr, M.; Knobler, C. B.; Diederich, F.; Wilkins, C. L. *J. Am. Chem. Soc.* **1991**, *113*, 495. (e) McElvany, S. W.; Ross, M. M.; Goroff, N. S.; Diederich, F. *Science* **1993**, *259*, 1594. (f) Diederich, F.; Rubin, Y.; Chapman, O. L.; Goroff, N. S. *Helv. Chim. Acta* **1994**, *77*, 1441.

(2) (a) Tobe, Y.; Fujii, T.; Matsumoto, H.; Naemura, K.; Achiba, Y.; Wakabayashi, T. *J. Am. Chem. Soc.* **1996**, *118*, 2758. (b) Tobe, Y.; Matsumoto, H.; Naemura, K.; Achiba, Y.; Wakabayashi, T. *Angew. Chem., Int. Ed. Engl.* **1996**, *35*, 1800. (c) Tobe, Y.; Fujii, T.; Matsumoto, H.; Tsumuraya, K.; Noguchi, D.; Nakagawa, N.; Sonoda, M.; Naemura, K.; Achiba, Y.; Wakabayashi, T. *J. Am. Chem. Soc.* **2000**, *122*, 1762. (d) Tobe, Y.; Umeda, R.; Iwasa, N.; Sonoda, M. *Chem. - Eur. J.* **2003**, *9*, 5549.

(3) Adamson, G. A.; Rees, C. W. *J. Chem. Soc., Perkin Trans. 1* **1996**, 1535.

(4) von Helden, G.; Gotts, N. G.; Bowers, M. T. *Nature* **1993**, *363*, 60.

(5) Crowley, J. D.; Goldup, S. M.; Lee, A. L.; Leigh, D. A.; McBurney, R. T. *Chem. Soc. Rev.* **2009**, *38*, 1530.

(6) (a) Saito, S.; Takahashi, E.; Nakazono, K. *Org. Lett.* **2006**, *8*, 5133. (b) Sato, Y.; Yamasaki, R.; Saito, S. *Angew. Chem., Int. Ed.* **2009**, *48*, 504. (c) Hayashi, R.; Wakatsuki, K.; Yamasaki, R.; Mutoh, Y.; Kasama, T.; Saito, S. *Chem. Commun.* **2014**, *50*, 204. (d) Yamashita, Y.; Mutoh, Y.; Yamasaki, R.; Kasama, T.; Saito, S. *Chem. - Eur. J.* **2015**, *21*, 2139.

(7) (a) Berná, J.; Goldup, S. M.; Lee, A.-L.; Leigh, D. A.; Symes, M. D.; Teobaldi, G.; Zerbetto, F. *Angew. Chem., Int. Ed.* **2008**, *47*, 4392. (b) Goldup, S. M.; Leigh, D. A.; Long, T.; McGonigal, P. R.; Symes, M. D.; Wu, J. *J. Am. Chem. Soc.* **2009**, *131*, 15924.

(8) Langton, M. J.; Matichak, J. D.; Thompson, A. L.; Anderson, H. L. *Chem. Sci.* **2011**, *2*, 1897.

(9) Movsisyan, L. D.; Kondratuk, D. V.; Franz, M.; Thompson, A. L.; Tykwinski, R. R.; Anderson, H. L. *Org. Lett.* **2012**, *14*, 3424.

(10) (a) Weisbach, N.; Baranova, Z.; Gauthier, S.; Reibenspies, J. H.; Gladysz, J. A. *Chem. Commun.* **2012**, *48*, 7562. (b) Baranová, Z.; Amini, H.; Bhuvanesh, N.; Gladysz, J. A. *Organometallics* **2014**, *33*, 6746.

(11) Movsisyan, L. D.; Franz, M.; Hampel, F.; Thompson, A. L.; Tykwinski, R. R.; Anderson, H. L. *J. Am. Chem. Soc.* **2016**, *138*, 1366.

(12) Franz, M.; Januszewski, J. A.; Wendinger, D.; Neiss, C.; Movsisyan, L. D.; Hampel, F.; Anderson, H. L.; Görling, A.; Tykwinski, R. R. *Angew. Chem., Int. Ed.* **2015**, *54*, 6645.

(13) Schrettl, S.; Contal, E.; Hoheisel, T.; Fritzsche, M.; Balog, S.; Szilluweit, R.; Frauenrath, H. *Chem. Sci.* **2015**, *6*, 564.

(14) (a) Roche, C.; Sour, A.; Niess, F.; Heitz, V.; Sauvage, J. P. *Eur. J. Org. Chem.* **2009**, *2009*, 2795. (b) Roche, C.; Sauvage, J.-P.; Sour, A.; Strutt, N. L. *New J. Chem.* **2011**, *35*, 2820.

(15) (a) Megiatto, J. D.; Schuster, D. I. *Org. Lett.* **2011**, *13*, 1808. (b) Megiatto, J. D.; Schuster, D. I.; de Miguel, G.; Wolfrum, S.; Guldi, D. M. *Chem. Mater.* **2012**, *24*, 2472.

(16) Chalifoux, W.; Tykwinski, R. R. *Nat. Chem.* **2010**, *2*, 967.

(17) Single-crystal X-ray diffraction data for **Zn-P3Ra** were collected with synchrotron radiation using I19 (EH1) at Diamond Light Source (λ = 0.6889 Å): Nowell, H.; Barnett, S. A.; Christensen, K. E.; Teat, S. J.; Allan, D. R. *J. Synchrotron Radiat.* **2012**, *19*, 435. Cell parameters were determined and refined and raw frame data were integrated using CrysAlisPro (Agilent Technologies, 2010). The structure was solved with SuperFlip: Palatinus, L.; Chapuis, G. *J. Appl. Crystallogr.* **2007**, *40*, 786. It was then refined by full-matrix least-squares on F^2 using CRYSTALS: Betteridge, P. W.; Carruthers, J. R.; Cooper, R. I.; Prout, K.; Watkin, D. J. *J. Appl. Crystallogr.* **2003**, *36*, 1487. Cooper, R. I.; Thompson, A. L.; Watkin, D. J. *J. Appl. Crystallogr.* **2010**, *43*, 1100. Parois, P.; Cooper, R. I.; Thompson, A. L. *Chem. Cent. J.* **2015**, *9*, 30. The structure contains large solvent-accessible voids comprising weak, diffuse electron density which were treated using PLATON/SQUEEZE: Spek, A. *J. Appl. Crystallogr.* **2003**, *36*, 7. van der Sluis, P.; Spek, A. L. *Acta Crystallogr., Sect. A: Found. Crystallogr.* **1990**, *46*, 194. Single Crystal Data: $C_{301}H_{348}N_8O_{17}Zn$, M_r = 4415.49, monoclinic, *Pc*; *a* = 31.7209(5) Å, *b* = 19.3373(2) Å, *c* = 50.4748(7) Å, β = 96.0619(14)°, *V* = 30787.9(7) Å, data/restraints/parameters: 52640/18794/5933, R_{int} = 6.99%, final R_1 = 12.36%, wR_2 = 31.63% ($I > 2\sigma(I)$), $\Delta\rho_{min,max}$ = −0.78, +0.88 e Å^3. Crystallographic data (excluding structure factors) have been deposited with the Cambridge Crystallographic Data Centre (CCDC 1519120); copies of these data can be obtained free of charge via www.ccdc.cam.ac.uk/data_request/cif.

(18) Movsisyan, L. D.; Peeks, M. D.; Greetham, G. M.; Towrie, M.; Thompson, A. L.; Parker, A. W.; Anderson, H. L. *J. Am. Chem. Soc.* **2014**, *136*, 17996.

(19) Lucotti, A.; Tommasini, M.; Fazzi, D.; Del Zoppo, M.; Chalifoux, W. A.; Ferguson, M. J.; Zerbi, G.; Tykwinski, R. R. *J. Am. Chem. Soc.* **2009**, *131*, 4239.

(20) (a) Szafert, S.; Gladysz, J. A. *Chem. Rev.* **2003**, *103*, 4175. (b) Szafert, S.; Gladysz, J. A. *Chem. Rev.* **2006**, *106*, PR1.

DOI: 10.1021/acs.orglett.6b03528
Org. Lett. 2017, 19, 348−351